Modeling macroalgae growth and nutrient dynamics for integrated multi-trophic aquaculture

Article *in* Journal of Applied Phycology · April 2014

DOI: 10.1007/s10811-014-0370-y

4 authors:

Scott Hadley
University of Tasmania
9 PUBLICATIONS **103** CITATIONS
SEE PROFILE

Karen wild-allen
The Commonwealth Scientific and Industrial Research Organisation
39 PUBLICATIONS **797** CITATIONS
SEE PROFILE

Craig R Johnson
University of Tasmania
254 PUBLICATIONS **11,815** CITATIONS
SEE PROFILE

Catriona K Macleod
University of Tasmania
66 PUBLICATIONS **1,477** CITATIONS
SEE PROFILE

Modeling macroalgae growth and nutrient dynamics for integrated multi-trophic aquaculture

Scott Hadley, Karen Wild-Allen, Craig Johnson & Catriona Macleod

Journal of Applied Phycology

ISSN 0921-8971

J Appl Phycol
DOI 10.1007/s10811-014-0370-y

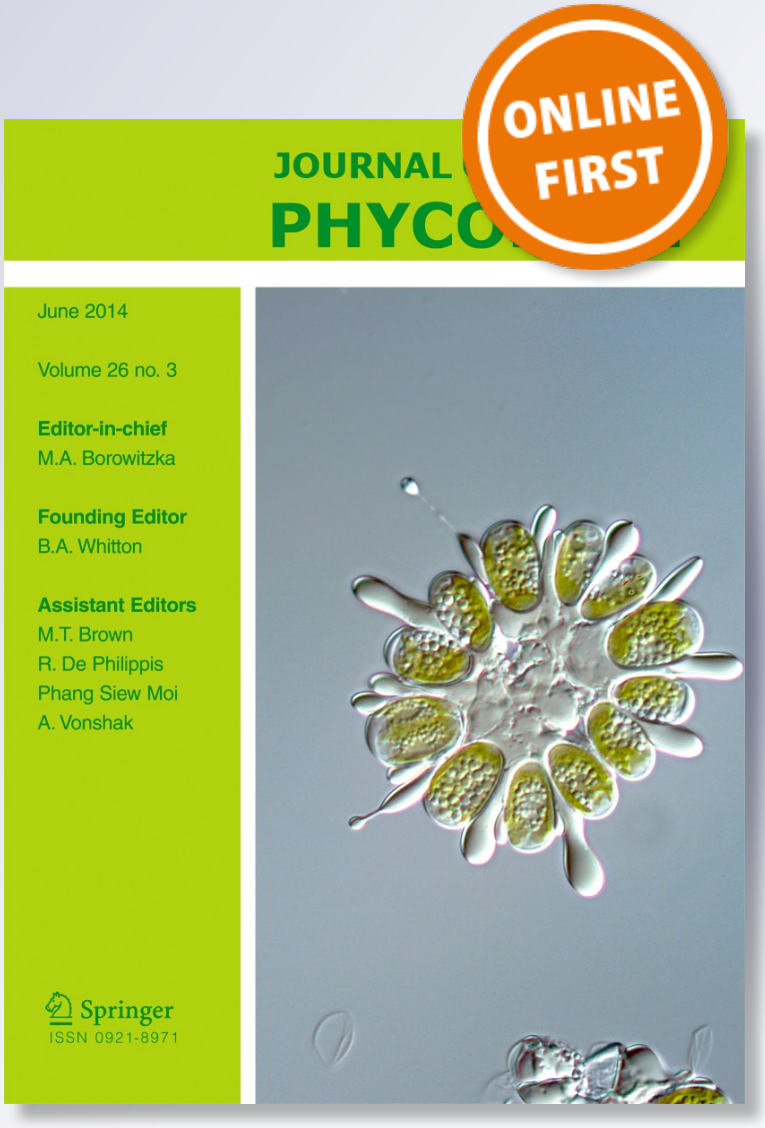

Springer

J Appl Phycol
DOI 10.1007/s10811-014-0370-y

Modeling macroalgae growth and nutrient dynamics for integrated multi-trophic aquaculture

Scott Hadley · Karen Wild-Allen · Craig Johnson · Catriona Macleod

Received: 2 March 2014 / Revised and accepted: 30 June 2014

Abstract Integrated multi-trophic aquaculture (IMTA) is being explored on both economic and environmental grounds in many traditional aquaculture regions. To test a variety of suitable macroalgae species and management scenarios, a numerical model is developed to quantify the remediation of dissolved nutrients and production of macroalgae near a nutrient source. Differences in the morphological, physiological, and economic characteristics of different macroalgae species can provide flexibility when considering the cost and benefit of farming macroalgae. Results show that of the three species studied, *Macrocystis pyrifera* removed 75 % of dissolved inorganic nitrogen (DIN) input from a point source, while *Porphyra umbilicalis* and *Ulva lactuca* removed 5 %. Both *M. pyrifera* and *P. umbilicalis* have reduced bioremediation capacity at increasing flow rates. *U. lactuca* showed increased bioremediation potential as flow rate increased from low to moderate flows. Increasing the optical depth increased the bioremediation potential of *M. pyrifera* for moderate values of the light attenuation coefficient, whereas bioremediation was unaffected by optical depth for both *U. lactuca* and *P. umbilicalis*. Harvesting increased bioremediation capacity of all species by up to 25-fold dependent on the establishment phase and harvesting frequency. We conclude that the choice of macroalgae species greatly affects the success of IMTA and that both harvesting and farm arrangements can be used to greatly optimize bioremediation.

S. Hadley (✉) · C. Johnson · C. Macleod
Institute for Marine and Antarctic Studies, University of Tasmania, Private Bag 129, Hobart, Tasmania 7001, Australia
e-mail: scott.hadley@csiro.au

K. Wild-Allen
CSIRO Marine and Atmospheric Research, GPO Box 1538, Hobart, Tasmania 7001, Australia

Published online: 12 July 2014

Keywords IMTA · *Macrocystis* · *Ulva* · *Porphyra* · Bioremediation · Temperate estuary · Management

Introduction

An important potential environmental impact of salmonid farming is the accumulation of waste products in the waterway. In estuaries where water circulation may be restricted, there is a possibility that the accumulation of farm waste will form a nutrient-rich system with a resultant shift in trophic status (Wild-Allen et al. 2010). Integrated multi-trophic aquaculture (IMTA), which involves farming of fed species like finfish together with "extractive" species such as seaweeds and filter feeders to take up inorganic and organic nutrients, respectively, has the potential to mitigate the environmental impacts of salmon aquaculture (Buschmann et al. 2008).

The extractive species can have economic value in their own right. IMTA takes a more balanced "whole-of-ecosystem" approach to management and typically takes into consideration site specificity, operational limits, revenues, and food safety guidelines, as well as environmental quality and regulations (Troell et al. 2009). There have already been several empirical studies into the effects of the nutrient output from fish farms on the growth of macroalgae (Buschmann et al. 2008; Hernandez et al. 2005; Sanderson et al. 2008). These studies found that macroalgae biomass increased in the presence of the fish farms but concluded that more detailed studies were needed to model nutrient dynamics, optimize farm design, and identify suitable seaweed species—all which may be site-specific. Empirical studies have been conducted to show comparisons between different species in the filtration of dissolved inorganic nitrogen (DIN) from fish effluent (Hernandez et al. 2002; 2005). However, these studies were conducted in tanks and plant morphology was not considered.

Results from small-scale systems do not necessarily extrapolate to large-scale operations because the removal of nutrients involves non-linear interactions between many variables. A modeling approach can help to understand these interactions, as full-scale trial operations may be prohibitively expensive. Models have been used to quantify the potential benefits of IMTA in an existing aquaculture system (Broch et al. 2013; Ren et al. 2012; Silva et al. 2012); however, in these studies, the assessment of macroalgae was limited to one species. Buschmann et al. (2008) showed that two commercial macroalgae species in Chile had similar bioremediative potential, but at differing cultivation depths. This has significant implications for any potential farming operation. A key goal in implementing IMTA is to optimize the ratio of fed to extractive species (based on local hydrodynamic, physical, and chemical water quality characteristics) to maximize the overall cost-benefit ratio. Another key goal is to identify an optimal harvesting strategy. Frequent harvesting enables constant removal of nutrients from the water (Chopin et al. 1999), but harvest strategies have to guarantee an increase in bioremediation and need to be balanced by economic considerations.

Species previously identified as most suitable for IMTA are those that are at their most productive in summer, have high rates of nutrient uptake (and thus high growth rates), have economic value in their own right, and are easily cultivated (Troell et al. 2009). Identifying suitable seaweed species and determining farm design to optimize the impact and economic return of IMTA will be aided greatly by development of suitable models that can be applied readily to locations anywhere in the world.

In this paper, we apply a macroalgae growth model to compare the bioremediation capacity of three species of macroalgae in a flexible IMTA environment. Using a set of scenarios, we examine the effect of variation in ammonium loads, refresh rate, optical depth, and harvesting schemes on the seasonal yield of macroalgae.

Model description

The macroalgae growth model we used here is based on those originally described by Solidoro et al. (1997) and Aldridge and Trimmer (2009). We have introduced a term for the increase in height of *Macrocystis pyrifera* (Phaeophyceae) based on biomass. We can use this term to assess the potential difference between kelp and smaller macroalgae grown for the purposes of IMTA. We are simulating a mesocosm, which represents a macroalgae farm with a salmon farm point source inputting a nitrogen load into the farm volume. Here, we present a brief description of the state equations; more detailed processes and parameter information is included in Table 4 the Appendix.

Dissolved inorganic nitrogen (DIN) is modeled in two forms: nitrate (NO_3; mg N m^{-3}) and ammonium (NH_4; mg N m^{-3}) (Fig. 1). This allows distinguishing the output from the salmon farms, which is largely in the form of ammonium (~97 % of ammonia derived from the salmon is assumed to be protonated to ammonium instantly), from background concentrations of ammonium and nitrate. The currency of N is chosen for this study because this nutrient limits autotroph growth in the region (Thompson et al. 2005). Dissolved inorganic phosphorous (DIP) is a potentially limiting nutrient in estuarine systems; however, it is also output as waste from the salmon farms. The ratio of DIN to DIP output from salmon farms ranges from 5:1 to 12:1 (mol:mol) (Wang et al. 2012; Wild-Allen et al. 2010) which is well below the Redfield ratio of 16:1 and Atkinson ratio 30:1 for phytoplankton and benthic marine plant tissue composition. We therefore assume DIN remains in shortest supply and is the limiting nutrient in proximity to the fish farms.

The total concentration of DIN in the water passing through the macroalgae farm is calculated from the combination of the concentration of the inflow at the background reference concentration, NX_{xref}, and the outflow at the macroalgae farm's internal concentration, NX_x. There are internal DIN losses due to farmed macroalgae as well as transformations due to the processes of nitrification and remineralization and an input of ammonia from the salmon farm, which gives:

$$V_{\mathrm{farm}}\frac{\mathrm{dNH_4}}{\mathrm{dt}} = F_{\mathrm{in}}\mathrm{NH_{4ref}} - F_{\mathrm{out}}\mathrm{NH_4} - f(\mathrm{NH_4},\mathrm{Q})BV_{\mathrm{MA}} + \mathrm{Fish_{in}} + V_{\mathrm{farm}}r_{\mathrm{L}}D - V_{\mathrm{farm}}r_{\mathrm{N}}\mathrm{NH_4} \quad (1)$$

$$V_{\mathrm{farm}}\frac{\mathrm{dNO_3}}{\mathrm{dt}} = F_{\mathrm{in}}\mathrm{NO_{3ref}} - F_{\mathrm{out}}\mathrm{NO_3} - f(\mathrm{NO_3},\mathrm{Q})BV_{\mathrm{MA}} + V_{\mathrm{farm}}r_{\mathrm{N}}\mathrm{NH_4} \quad (2)$$

$V_{\mathrm{farm}}=zA_{\mathrm{farm}}$ is the volume of our macroalgae farm. Here, z is the cultivation depth and A_{farm} is the macroalgae farm area. Similarly, $V_{\mathrm{MA}}=h_{\mathrm{MA}}A_{\mathrm{farm}}$ is the volume occupied by the macroalgae (inside A_{farm}) with h_{MA} the height of the macroalgae in meters. In Eqs. (1) and (2), $F_{\mathrm{in}}=F_{\mathrm{out}}$ represents the flow rate through A_{farm}. B (Eq. (20) in Appendix) represents biomass, $f(NX_x,Q)$. Equation (12) controls the uptake rate of NX_x by macroalgae dependent on the internal quotient Q (Eq. (21) in Appendix). $\mathrm{Fish_{in}}$ is the point source input of NH_4 from the salmon farm into V_{farm}. The term $r_{\mathrm{L}}D$ represents the remineralization of detritus into NH_4. Finally, $r_{\mathrm{N}}\mathrm{NH_4}$ is the nitrification of ammonia to nitrate.

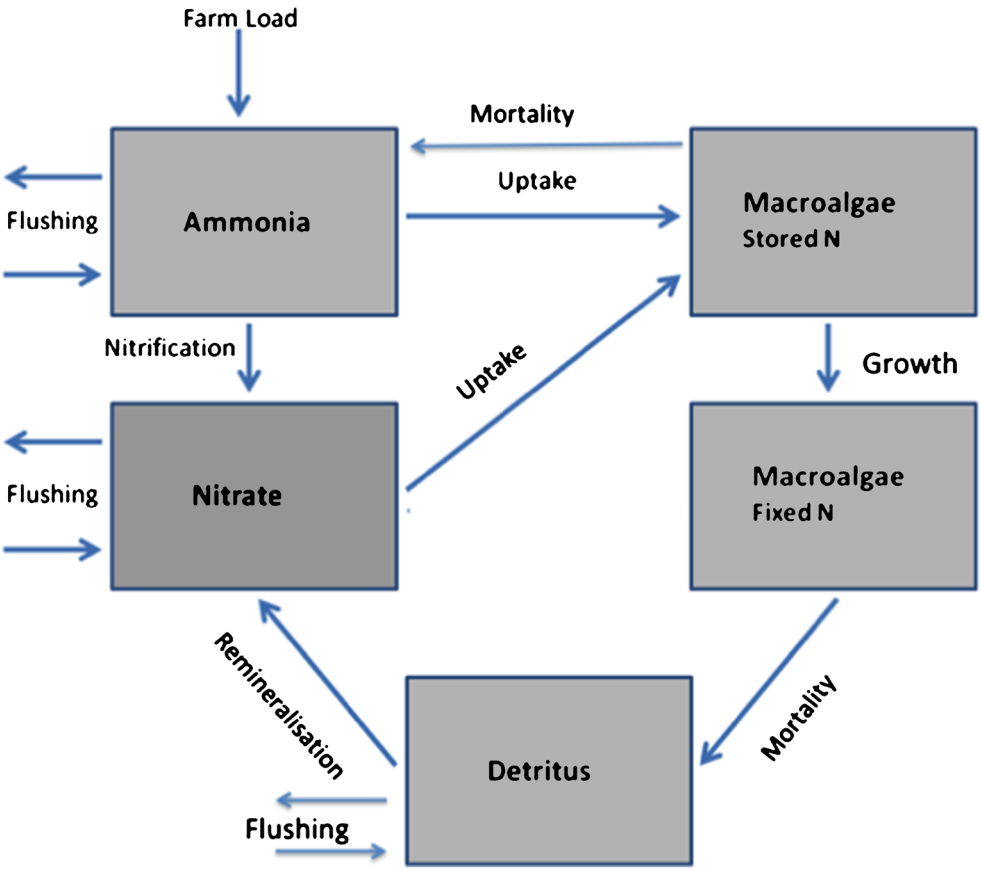

Fig. 1 Biogeochemical model of nutrient uptake by macroalgae. A load is placed on the system by the salmon farms in the form of dissolved ammonia. This is either absorbed by the algae or nitrified (to nitrate) in the water column. The algae have a two-step uptake process where nitrogen is first stored in intracellular pools and then assimilated into the alga's cellular structure at a rate dependent on environmental factors. Finally, the alga dies and fixed N is returned to detrital pools and stored N is returned to ammonia

In Eqs. (1) and (2), we divide through by V_{farm} to get

$$\frac{\mathrm{dNH_4}}{\mathrm{dt}} = \lambda_{\mathrm{R}}(\mathrm{NH_{4ref}} - \mathrm{NH_4}) - f(\mathrm{NH_4}, \mathrm{Q})B\left[\max\left(\frac{h_{\mathrm{MA}}}{z}, 1\right)\right] + N_{\text{farm}} + r_{\mathrm{L}}D - r_{\mathrm{N}}\mathrm{NH_4} \tag{3}$$

$$\frac{\mathrm{dNO_3}}{\mathrm{dt}} = \lambda_{\mathrm{R}}(\mathrm{NO_{3ref}} - \mathrm{NO_3}) - \mathrm{f}(\mathrm{NO_3}, \mathrm{Q})B\left[\max\left(\frac{h_{\mathrm{MA}}}{z}, 1\right)\right] + r_{\mathrm{N}}\mathrm{NH_4} \tag{4}$$

Here, λ_{R} is the refresh rate which is the ratio $F_{\text{in}}/V_{\text{farm}}$ and is a measure of how quickly the ambient nitrogen concentration inside V_{farm} returns to reference level without macroalgae present. We use this formulation (Aldridge and Trimmer 2009) to provide a method for examining effect of the flow rate on algae growth in the absence of an advection diffusion model. The default value for $\lambda_{\mathrm{R}}=0.25\ \mathrm{d}^{-1}$ is as used by Aldridge and Trimmer (2009), but we vary this parameter to examine the effect of flow rate on the algae growth. The term $\max\left(\frac{h_{\mathrm{MA}}}{z}, 1\right)$ is introduced in this model and determines the proportion of DIN the macroalgae can access in the farm volume (the maximum value of this term is 1 when macroalgae reaches the water surface). Finally, N_{farm} is the daily input of ammonia from the salmon farm averaged over our macroalgae farm volume.

In the model, the seaweeds *Ulva lactuca* (Chlorophyta) and *Porphyra umbilicalis* (Rhodophyta) are given a constant height, $h_{\mathrm{MA}}=0.2$ m, taken from literature values (Table 5). The giant kelp *M. pyrifera* (Phaeophyta) is allowed to change its height according to an allometric term, $h_{\mathrm{MA}}=(0.00174\mathrm{N_f}/\mathrm{num\_fronds})^{1.047}$ (Eq. (22) in the Appendix).

This term is derived from the work by Utter and Denny (1996) relating frond mass to height for *M. pyrifera*. In our model, we determine the mass per square meter of macroalgae, but not the number of fronds within this area. We introduced the parameter num_fronds to represent the average number of *M. pyrifera* fronds in an area, where we are assuming that a plant consists of several fronds all the same length h_{MA}. The value of num_fronds=7 was determined through model calibration to ensure the *M. pyrifera* height increased at a realistic rate. The increase in height of the kelp effectively increases both its exposure to the DIN passing through the farm volume and its access to light.

Macroalgae growth is modeled as a two-step process. First, DIN is taken up into intracellular pools as an internal reserve of stored nitrogen (N_s; mg N m^{-3}), and then N_s is converted into fixed nitrogen (N_f; mg N m^{-3}), resulting in increased macroalgae biomass B. The uptake of N_s is observed to be independent of light (Aldridge and Trimmer 2009) and is modeled as dependent on the external concentration of DIN (ammonia and nitrate) and the internal nitrogen quota Q. The conversion of N_s to N_f (growth) is dependent on internal reserves, light, and temperature.

$$\frac{dN_s}{dt} = f(NX_x, Q)B\max\left(\frac{h_{MA}}{z}, 1\right) - \mu g(E, Q, T)N_s - d_M N_s \quad (5)$$

$$\frac{dN_f}{dt} = \mu g(E, Q, T)N_s - d_M N_f \quad (6)$$

In Eqs. (5) and (6), $\mu g(E, Q, T)$ (Eq. (13)) represents the growth function for macroalgae dependent on light (E), internal nutrient reserves (Q), and temperature (T), while $d_M N_s$ and $d_M N_f$ are mortality terms. The breakdown of macroalgal tissue forms detritus (D; mg N m^{-3}), with subsequent remineralization of D back to NH_4 as well as release of N_s (from lost tissue) as NH_4. We also model the loss of detritus from the farm volume, with D_{ref} the background concentration of the natural system.

$$\frac{dD}{dt} = \lambda_R(D_{ref} - D) + d_M N_f - r_L D \quad (7)$$

Equations (3)–(7) form the state equations for our system.

The environment

We force the model with a seasonal cycle of irradiance, temperature, and nutrients, using the functional form,

$$X = X_{av} + SD \times \sin\left(\frac{2\pi t}{365} + t_s\right) \quad (8)$$

Here, X is the instantaneous value of one of the environmental variables, X_{av} is the annual mean, SD is the standard deviation from the annual mean, t is time (days), and t_s (days) controls the phase shift of the sine function (nutrients have peak concentrations in winter, while photosynthetically active radiation (PAR) and temperature have peak values in summer). The values for temperate Australian waters were obtained from the CSIRO Atlas of Regional Seas (CARS) database (CSIRO 2009) for (approximate) latitude 43.0902 (S) and longitude 147.0231 (E) (Fig. 2).

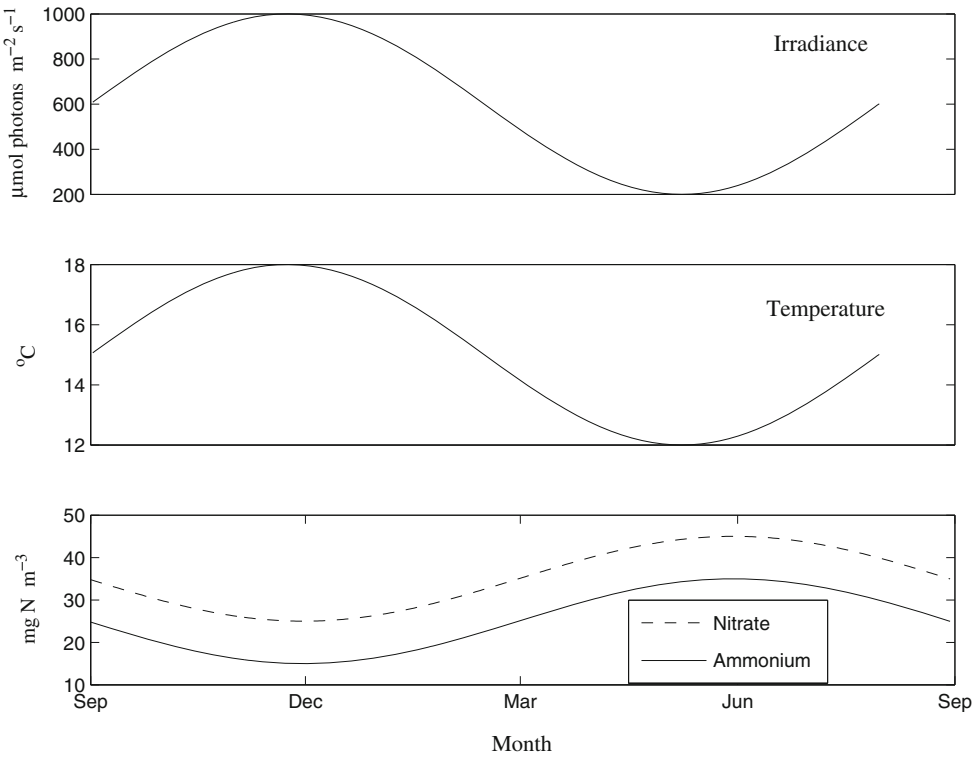

Fig. 2 The irradiance is PAR and is approximated by a smooth function, to represent the range and seasonal strength typical of the region, with a peak in summer months. This is the same seasonal signal for sea temperature. Ambient nitrate and ammonia (NX_x) are highest in winter

Macroalgae species

The three species of macroalgae selected for comparison (*U. lactuca*, *P. umbilicalis*, and *M. pyrifera*) all occur naturally in southeast Tasmanian waters of Australia (Sanderson and Di Benedetto 1988) and are suited to the local conditions, which is an important factor in choosing a suitable species (Carmona et al. 2006). All three have both high growth rates and low nitrogen storage capacity. Each of these species has been tested experimentally for potential in IMTA (Buschmann et al. 2008; Carmona et al. 2006; Yokoyama and Ishihi 2010) with encouraging results.

U. lactuca, *P. umbilicalis*, and *M. pyrifera* differ in their economic value, bioremediation potential, and conservation value to the natural ecosystem. The potential growth of each species is distinguished in our model by the individual species parameters (Table 5, Appendix). We also differentiate between the smaller seaweeds *U. lactuca* and *P. umbilicalis* (height=0.2 m), and the giant kelp *M. pyrifera* (variable height). We use this variation in height to investigate how kelp optimizes its light environment and increases its nutrient capturing capacity in contrast to the smaller species that do not have the ability to grow over a large range of heights.

Model simulations

All model simulations described in this section are run over a growing season of 365 days (unless otherwise stated) beginning in spring (September).

General behavior

The following simulations are designed to establish the general behavior of our model. Firstly, we conduct a reference run using the parameter values specified in Table 5 for each algal species and the environmental forcing outlined in "The environment". The reference level of input of ammonium from the salmon farms is set at $N_{\text{farm}}=100\text{mg N m}^{-3}\text{d}^{-1}$. We use this reference run to establish the bioremediation capacity of each species under "typical" site conditions. We then look at the effect that changing the ammonium output from the salmon aquaculture has on the model results. We use two values of $N_{\text{farm}}=50\,\text{and}\,100\text{ mg N m}^{-3}\text{d}^{-1}$, run the model forward until steady state is reached, and then compare the results for our two values. Finally, we run the model with $N_{\text{farm}}=5{,}000\text{ mg N m}^{-3}\text{d}^{-1}$ so that growth achieves steady state due to light limitation (nutrient replete system) and analyze the results.

Model validation

The purpose of this study is to apply a macroalgae model to compare the growth/bioremediation capacity of three different species of macroalgae in an IMTA environment. In order to validate our results, we need to offer evidence that the model is able to offer reasonable simulations of macroalgae growth for all of three species examined. This gives us confidence in the results from the simulations carried out in our comparison study. We establish the fitness of purpose of our model by comparing model growth rates against those published in empirical studies on IMTA for each algal species. To do this, we use the environmental forcing, DIN loads, and growth period outlined in each empirical study in our model setup and compare the growth rates predicted by our model results with the literature values according to the formula,

$$\text{SGR} = 100 \times \ln(w_t - w_o)/t \tag{9}$$

Where w_o is the initial weight of the macroalgae and w_t is weight at the end of the growing period t.

Sensitivity analysis

To determine the sensitivity of the model to changes in a parameter value, we perturb each parameter in turn by 10 % and assess the sensitivity according to

$$\text{Sensitivity} = \frac{(V(1.1p) - V(0.9p))}{0.2V(p)} \tag{10}$$

where $V(p)$ is the output from the model with a parameter value equal to p and $V(1.1p)$ and $V(0.9p)$ represent the model output with the parameter equal to 110 and 90 % of the value of p, respectively (Everett et al. 2007). This normalized relative sensitivity (Eq. (10)) is equivalent to the relationship

$$\frac{\Delta \ln(V(p))}{\Delta \ln(p)} \tag{11}$$

so that sensitivity=2 implies $V(p) \propto p^2$ and therefore a doubling of the parameter value p results in $V(2p) \propto 4p^2$, i.e., a fourfold increase in output.

Flow rate

In the model, refresh rate is used as a proxy for flow, and thus, by varying λ_R, we can investigate the effect of changing the flow rate on the model state variables for each species. In this simulation, we run the model using the reference values

established in "General behavior" with the exception that we vary the value of the refresh rate parameter. We use two values of the refresh rate parameter, the first, λ_R=0.05 d^{-1}, represents a fivefold decrease in the reference value given in Table 5 (λ_R=0.25 d^{-1}) and this represents low flow conditions (in this simulation). The second value, λ_R=1.0 d^{-1}, is a fourfold increase in the reference value and is representative of higher flow conditions. We then compare the model results to assess the effect of flow rate on system dynamics.

Optical depth

Optical depth is the product of the actual cultivation depth z and the light attenuation coefficient of the water K_d. For this simulation, we keep z constant at 3 m and vary K_d. We set the reference value for K_d=0.1 m^{-1} (Table 5) which is equivalent to the background light attenuation coefficient of clear seawater (K_w). In this simulation, we include attenuation due to colored dissolved organic matter (CDOM) (we are not considering phytoplankton in this study). Light attenuation due to CDOM in the Huon Estuary in Tasmania (site of the environmental forcing in "The environment") can range between 0.1 and 6.0 m^{-1} for surface water and 0.1 and 2.0 m^{-1} at a depth of 3 m (Clementson et al. 2004). We examine the response of each species to a change in the light field by running the model for varying K_d (0.2, 0.6, and 1.0 m^{-1}) and compare the model results.

Harvesting

We assess the effect of harvesting algal biomass on the model results for each species. Thinning of crops is a common farming practice that optimizes growth by reducing the limiting effects of self-shading. Harvesting can also be imposed by the economic demand of market supply. In practice, *P. umbilicalis* has been traditionally left for an initial phase of 5 months and then harvested at two weekly intervals, while *U. lactuca* has a lifespan of approximately 3 months (ElkhornSlough.org 2012) and so must be harvested more regularly. Giant kelp fronds typically have a lifespan of at least 6 months (North et al. 1986), whereas *P. umbilicalis* can live at least a whole season (MarLIN 2012).

We define a harvesting scheme as establishment phase and harvest frequency. The establishment phase is the period that macroalgae is grown before harvesting commences. The harvesting frequency is the time between harvests. "Harvest amount" is the percentage of total macroalgae in the farm that is taken per harvest. We have constructed nine schemes (Table 1) varying in establishment phase and harvesting frequency. Each scheme incorporates the lifespan of the species being harvested and ensures that there is no harvest interval greater than the maximum age of a frond so that we can discount natural losses due to senescence.

Table 1 A harvesting scheme is defined by the establishment period and harvesting frequency

Scheme	Establishment period (days)	Harvest frequency (days)
1	30	14
2	30	28
3	30	90
4	60	14
5	60	28
6	60	90
7	90	14
8	90	28
9	90	90

The three establishment periods and three harvesting frequencies combine to form the nine schemes we examined

For each scheme, the model is run forward until t=establishment phase (est) days. We then remove a fraction H=0.2 (25 %) of both $N_f(t$=est) and $N_s(t$=est) and restart the model with new initial conditions [$NH_4(t$=est);NO_3(est); (1−H)N_s(est);(1−H)N_f(est); D(est)]. We repeat this process running the model forward for each harvesting (har.) period and removing the same proportion of N_f and N_s until the end of the season. The accumulated total of removed N_f+ N_s is added to the end of season amount of N_f+ N_s to give a total N for each scheme. We repeat the simulation for H=0.5, i.e., a 50 % removal rate. The simulations for *M. pyrifera* are conducted so that the plants are thinned with no reduction in height (and height is constant for the other species). Model runs are conducted for each species at the reference values.

Simulation results

All state variables are presented in terms of mass per area rather than mass per volume for easier interpretation of the results. We define the following terms used in this section:

fixed N=$N_f \times h_{MA}$ (mg N m^{-2}), stored N=$N_f \times h_{MA}$ (mg N m^{-2}), and total N removed=fixed N+stored N, which is the total amount of nitrogen removed by the macroalgae per unit area of the macroalgal farm.

General behavior

We completed a reference run (outlined in "General behavior") for each species. From the model results, we calculated the daily accumulated N per unit area of macroalgae farm input from the salmon aquaculture activity as accumulated N = $N_{farm}tz$ (mg N m^{-2}). We then compared total N removed, accumulated N, and the difference (accumulated N−total N removed) for each

species (Fig. 3). These results show the bioremediative capacity of each species at a reference site by directly comparing the amount of N put into the system by aquaculture with the amount removed by the macroalgae. This shows that *M. pyrifera* is able to significantly impact the DIN from midsummer (Feb.). After April, the bioremediated input from the salmon farm no longer accumulates but instead reduces and eventually attains steady state (Fig. 3; dotted line) because the growth of the macroalgae is matching the input from the salmon farm (Fig. 3a; solid line). End-of-season values for the accumulated N and accumulated N−total N (Fig. 3; dashed versus dotted lines) indicate that *M. pyrifera* has removed approximately 75 % of the salmon farm output of DIN. Using the same comparison, *U. lactuca* and *P. umbilicalis* remove only approximately 5 % each.

If farm loads are increased, all three species eventually reach steady state (for all loads) after 10 years (Fig. 4). In the nutrient limited cases when N_{farm}=50 mg N $m^{-3}d^{-1}$ (solid line) and N_{farm}=100 mg N $m^{-3}d^{-1}$ (dashed line), respectively, a doubling in farm load results in a doubling of end-of-season yield of fixed N. The trajectories of fixed N are similar for *U. lactuca* and *P. umbilicalis*, including similar final steady-state values at all rates of farm input. The final fixed N for the *M. pyrifera* is an order of magnitude (×10) larger than those obtained by the smaller species at the lower loads and double that of the other two species at the highest value of farm load. In the nutrient replete system (dotted line), model results gave the maximum end-of-season biomass for each species as *M. pyrifera* ~86–94 kg dw m^{-2}, *P. umbilicalis* ~23–26 kg dw m^{-2}, and *U. lactuca* ~24–27 kg dw m^{-2}.

Model validation

The specific growth rates (SGR) predicted by the model (Table 2) are similar to the results reported for each species from empirical experiments. The experiments with *P. umbilicalis* and *M. pyrifera* were conducted around fish farms, while the empirical work measuring the growth of *U. lactuca* was conducted in tanks using effluent from fish (Neori et al. 1991) and abalone (Robertson-Andersson et al. 2008) culture, respectively.

Sensitivity analysis

The model is relatively insensitive to the range of parameter values defining *U. lactuca* and *P. umbilicalis* (Table 3). For *M. pyrifera*, the model shows mild sensitivity to the parameters Q_{min}, I_s and K_c. Two of these are related to the internal storage capacity of *M. pyrifera* while the saturation constant dictates sensitivity to photoinhibition.

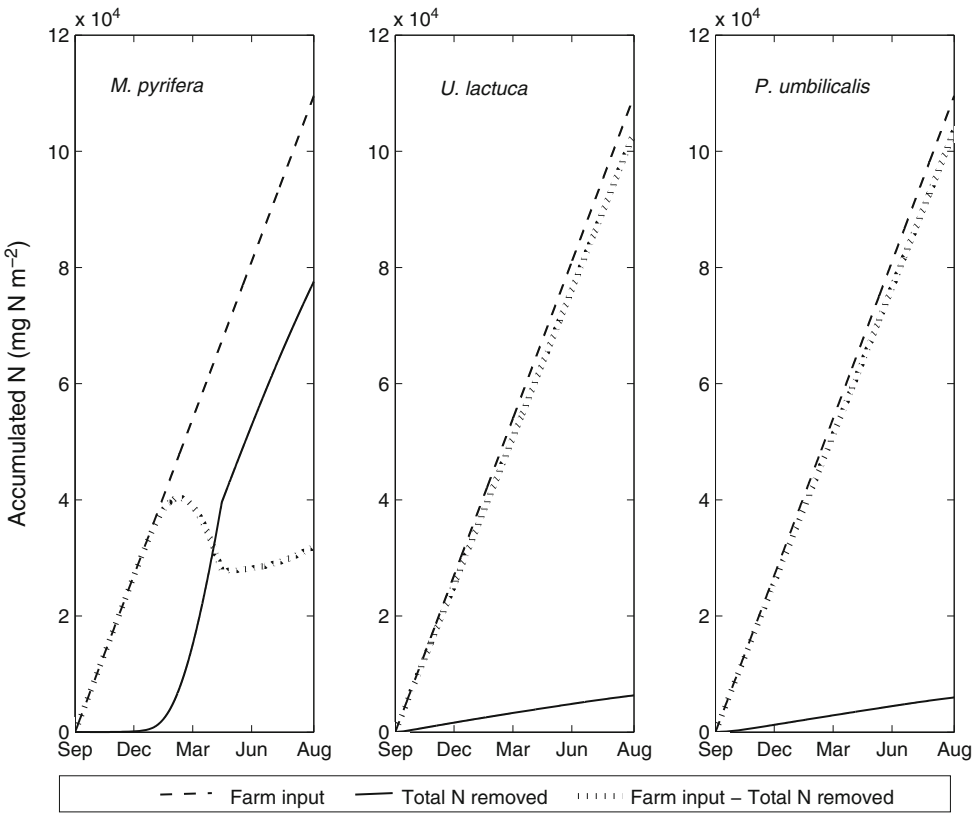

Fig. 3 The bioremediation of N_{farm} for each species per square meter of the macroalgae farm. The *dashed line* shows the farm input over a season per square meter. The *solid line* shows the total N removed by macroalgae per square meter, and the *dotted line* is the net N input into the system, i.e., farm input−total N removed by macroalgae. We multiplied N_{farm} by the water depth (z) to calculate the salmon load per square meter. Similarly, we multiplied (N_f+N_s) by the instantaneous height of the macroalgae (h_{MA}) to calculate the total N

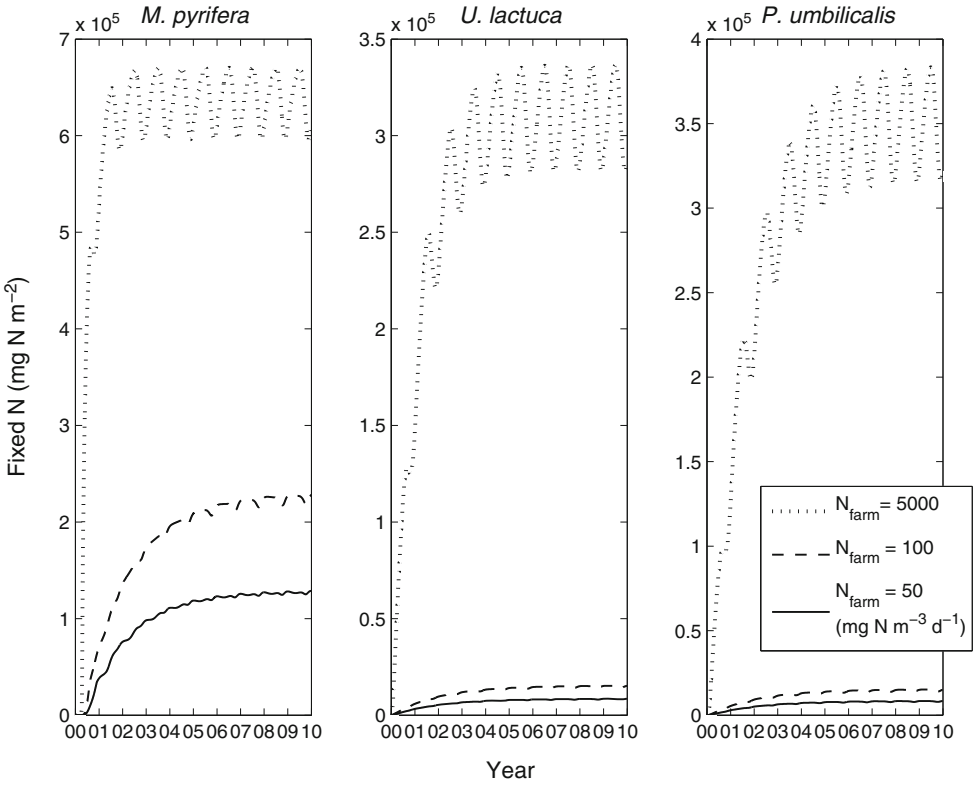

Fig. 4 The steady state of fixed N as we increase the value of N_{farm}. We multiply N_f by the instantaneous macroalgae height (h_{MA}) to calculate fixed N for each species per square meter. Only the value of N_{farm} is changed between model runs, and all other environmental forcing is kept at the reference level. Growth is eventually limited by the amount of N in the system for the two lower values of N_{farm}. At N_{farm}= 5,000 mg N m^{-3} d^{-1}, we are simulating a nutrient replete system where growth is eventually limited by light for all three species

Flow rate

At the lower flow rate, *M. pyrifera* and *P. umbilicalis* achieve consistently higher remediation over the whole season than that achieved at the higher flow (Fig. 5). This difference is greater for *P. umbilicalis* particularly at the end of the season where total N for *M. pyrifera* appears to converge for both values of λ_R. For *U. lactuca*, initially, total N increases at a faster rate in low flow conditions (compared with higher flow), but this rate slows and crosses the trajectory for total N under the higher flow conditions about mid season, then continues at a lower rate until the end of the season. Bioremediation capacity is slightly increased for *U. lactuca* under higher flow conditions.

Optical depth

Under low light, photosynthetic growth (fixed N) is less for *U. lactuca* and *P. umbilicalis* (Fig. 6) and growth strictly increases as light increases. For *M. pyrifera*, photosynthetic growth is lowest when the light is highest. This species also has the highest growth at the midrange of the optical depths examined. As the photosynthetic growth decreases, stored N increases for all three species. The net effect of this is an unchanged bioremediation capacity (total N) for both *U. lactuca* and *P. umbilicalis* across all optical depths examined. The bioremediation capacity of *M. pyrifera* is lowest in highest light and greatest at the midrange.

Table 2 Comparison of the growth rates as determined by the model result with that for the same species evaluated in a field-based IMTA experiment

Species	DIN μM	SGR % (g ww d^{-1})	Study
M. pyrifera	0.08–30	6 (t=9 months)	(Buschmann et al. 2008)
M. pyrifera	10–13	4	This study
U. lactuca	10–78	7.4–17.9 (t=2 weeks)	(Neori et al. 1991)
U. lactuca	5.0	1.6–6.3 (t=2 weeks)	(Robertson-Andersson et al. 2008)
U. lactuca	10–13	7	This study
P. umbilicalis	150	13.1 (t=4 weeks)	(Carmona et al. 2006)
P. umbilicalis	150	16	This study

All the studies define specific growth rate as SGR=100×ln(w_t−w_o)/t, where w_t and w_o are the weight of algae at time t and 0, respectively, and t is the growing period

Table 3 Sensitivity analysis results are based on a comparison of the end of season total of N_f using Eq. (9)

M. pyrifera		*U. lactuca*		*P. umbilicalis*	
Parameter	Sensitivity	Parameter	Sensitivity	Parameter	Sensitivity
Q_{min}	−0.82	d_M	−0.24	d_M	−0.23
I_s	0.53	r_L	0.11	Q_{min}	−0.18
K_c	0.44	Q_{min}	−0.10	r_L	0.10
K_d	0.29	T_0	−0.05	V_{NH_4}	0.09
d_M	−0.25	μ	0.05	μ	0.07

We show the five most sensitive parameters for each species where an absolute value of 0.3 is determined as the threshold for the model to be sensitive to the parameter. A negative value means total N_f decreases as the parameter increases

Harvesting

The results for all three species (Fig. 7) show that, compared with non-harvested crops, schemes with an establishment phase of 30 days result in a decrease in bioremediation (total N), 60 days result in an approximate doubling of bioremediation, and 90 days result in the greatest increase in bioremediation, but which varied greatly depending on harvest frequency. Across all schemes, total N increased with establishment phase and decreased with harvesting frequency. As the percentage removed (H) increased, total N removed increased for schemes with establishment phases of 90 days, but in the other schemes, the effect was negligible. For all macroalgae, schemes with a 90-day establishment period resulted in a 5–25-fold increase in bioremediation dependent on both harvesting frequency and H.

Discussion

General model behavior

An aim of the study was to quantify the bioremediation potential of three macroalgae species within the context of a modeling approach. The model indicates conclusively that of our three species, *M. pyrifera* is the most effective at removing the ammonia in a near field, i.e., 75 % of farm load, whereas the two smaller species remove only 5 % each. However, beginning the simulation in September, it took until March for *M. pyrifera* to better the removal rates of the other algae. Although we did not simulate phytoplankton in this study, in the natural environment, phytoplankton may remove the DIN before *M. pyrifera* is able to, thus reducing its growth and therefore its height and bioremediation capacity. Growing

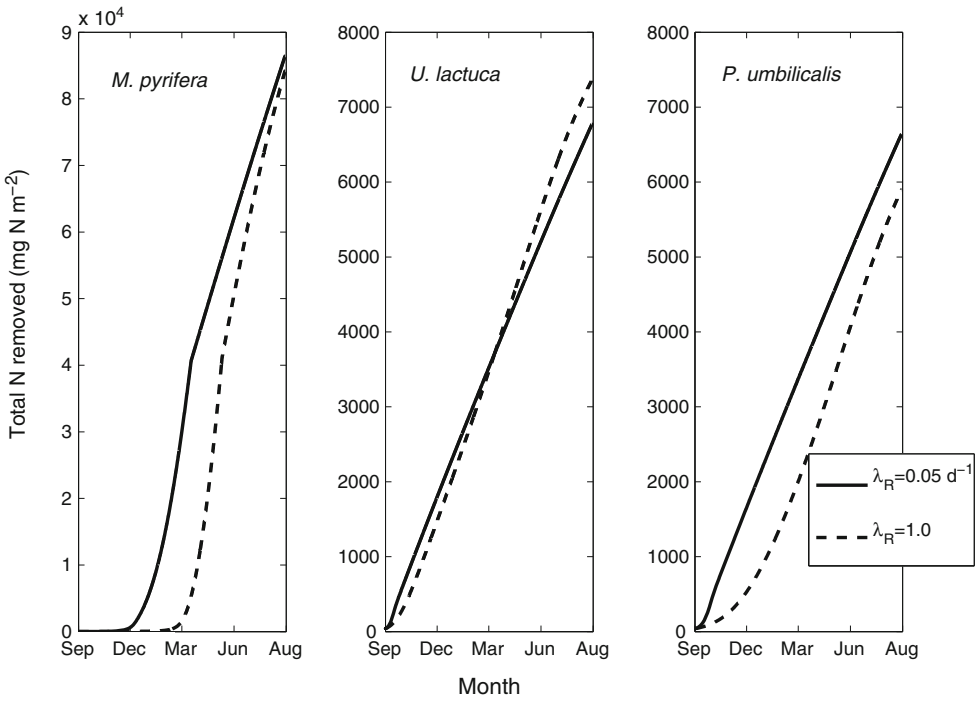

Fig. 5 Total N (=$(N_s+N_f)h_{MA}$) removal by per square meter by each species for two values of the refresh rate. By setting λ_R= 0.05 d^{-1} (*solid line*), we are simulating growth in low flow conditions. Setting λ_R=1.0 d^{-1} (a 20-fold increase in net flow) simulates higher flow conditions. All other environmental forcing is kept at the reference level

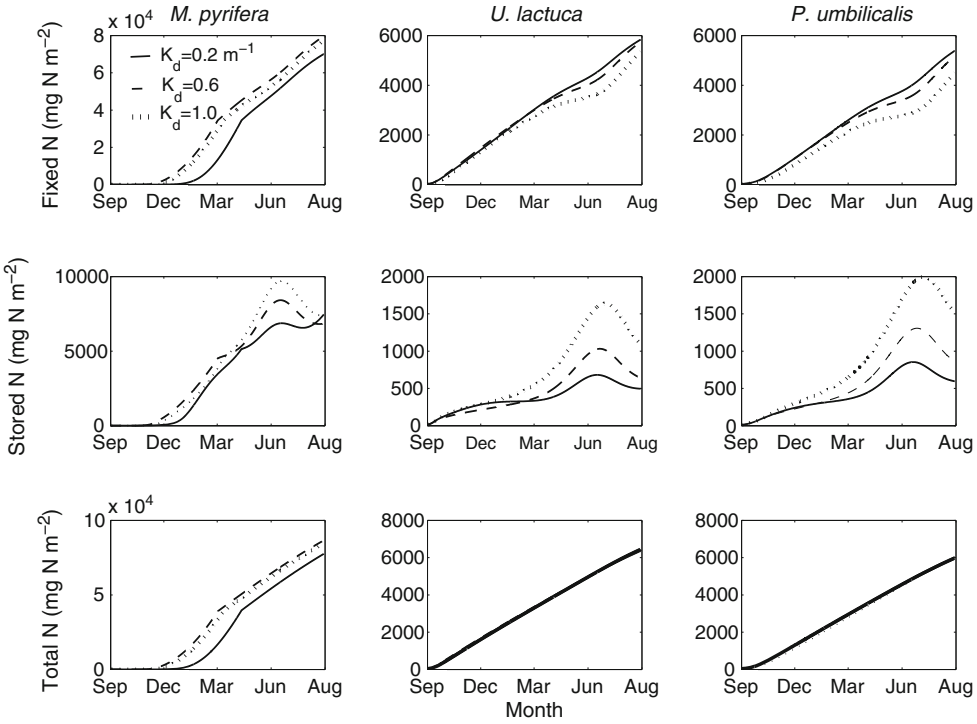

Fig. 6 Fixed N, stored N, and total N for each species at increasing values of the light attenuation coefficient K_d. The increase in K_d simulates increasing turbidity in the water column. Environmental forcing was kept at the reference level with only K_d varying

M. pyrifera earlier in the season may be an option as they may be at the height required to remove adequate quantities of DIN before phytoplankton become active (spring/summer). However, the light climate may not be adequate to achieve the growth rate required; in which case, growing kelps over consecutive seasons would seem a sensible solution. An obvious conclusion is that, in the near-field case, the height of macroalgae is a critical factor in its bioremediation potential. It may be possible to grow several of the smaller species on vertical lines to increase their vertical distribution.

Macroalgae growth reaches steady state due to nutrient limitation when $Q \sim Q_{min}$ at which point $N_s \sim 0$, i.e., stored nitrogen is close to 0. Theoretically, macroalgae could be grown in the long term around a constant N source and after a period (10 years in this case) it would match its growth exactly to the input source to achieve a system in equilibrium (although this does not take into account environmental losses, changes in seasonal cycle, and natural senescence). In the case of light limitation, the algae could not grow past a maximum biomass and its bioremediation capacity would have reached its upper limit. In this experiment, the simulated final biomass for all three species due to light limitation is *M. pyrifera* ~86–94 kg dw m^{-2}, *P. umbilicalis* ~24–27 kg dw m^{-2}, and *U. lactuca* ~23–26 kg dw m^{-2}. *U. lactuca* grown in a land-based IMTA facility demonstrated a production potential of 4.5 kg dw m^{-2} (Bruhn et al. 2011). It is therefore plausible that *U. lactuca* could reach the concentration found in this study before self-shading stops growth entirely. Although we have not found similar empirical results for our other two species, we interpret the results for *U. lactuca* as partial validation for the light component of the model.

Model validation

Similar formulations of the model used in this study have previously been validated against observation for different species of macroalgae (Aldridge and Trimmer 2009; Solidoro 1997). The results of our validation were conclusive in predicting growth rates achieved in field IMTA experiments for the species studied here. The model (Eqs. (3)–(7)) has been partially validated using a fitness for purpose criteria (Rykiel 1995).

Sensitivity analysis

The sensitivity analysis showed the model is not sensitive to parameter values in the range describing *U. lactuca* and *P. umbilicalis*. Our three species in effect represent a large perturbation of the parameter space, and it is encouraging to note that the model is not unduly sensitive across this perturbation which is evidenced by the fact that end-of-season N_f were similar across all species for each value of farm loading investigated. The model for *M. pyrifera* showed the greatest sensitivity to parameter perturbations, where Q_{min}, I_s and K_c all showed sensitivities above the 0.3 threshold ("Sensitivity analysis"). Firstly, the growth model had a slightly different formulation for *M. pyrifera*, where the h_{MA} varied. *M. pyrifera* has the lowest nitrogen storage capacity of the three species, and decreasing this capacity further decreases growth.

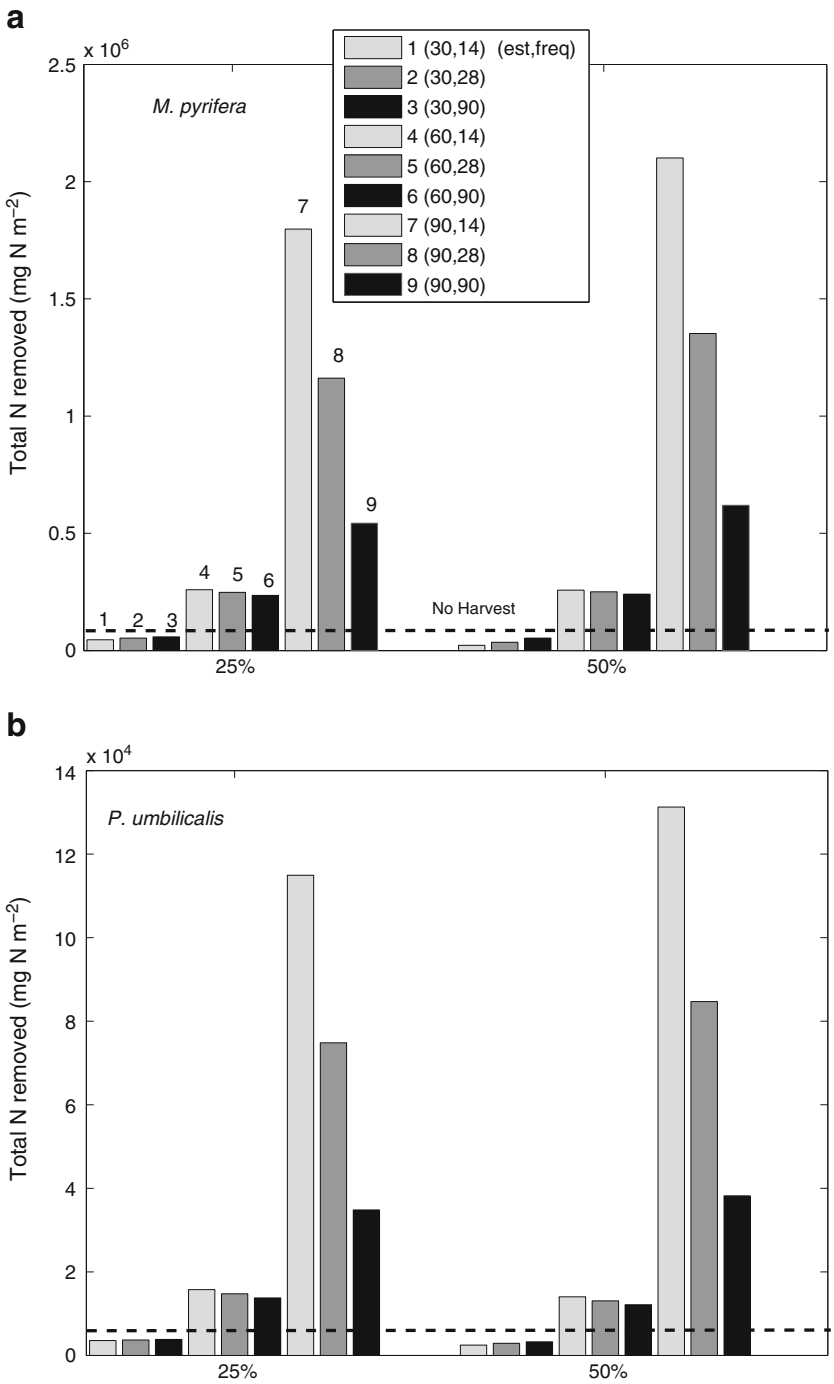

Fig. 7 Total N removed by each species. The total N removed is calculated for each harvesting scheme 1–9 with at first 25 % removed per harvest and then 50 %

Increasing K_c increases growth rate by allowing the macroalgae to fix a greater proportion of internal nitrogen before its growth is satiated. *M. pyrifera* is sensitive to photoinhibition in the field (Buschmann et al. 2008), and increasing I_s reduces this effect, i.e., increases growth rate. Overall, the model is not unduly sensitive; however, it is important to make parameters as realistic as possible to constrain model output to reasonable values.

Flow rate

The uptake of DIN into the macroalgae is modeled as dependent on biomass concentration (Eqs. (3) and (4)). As λ_R increases, so too does the rate at which N_{farm} is flushed out of the macroalgae farm. Conversely, the farm volume is being replenished by external DIN at an increasing rate. The net effect on bioremediation resulting from the increase in refresh

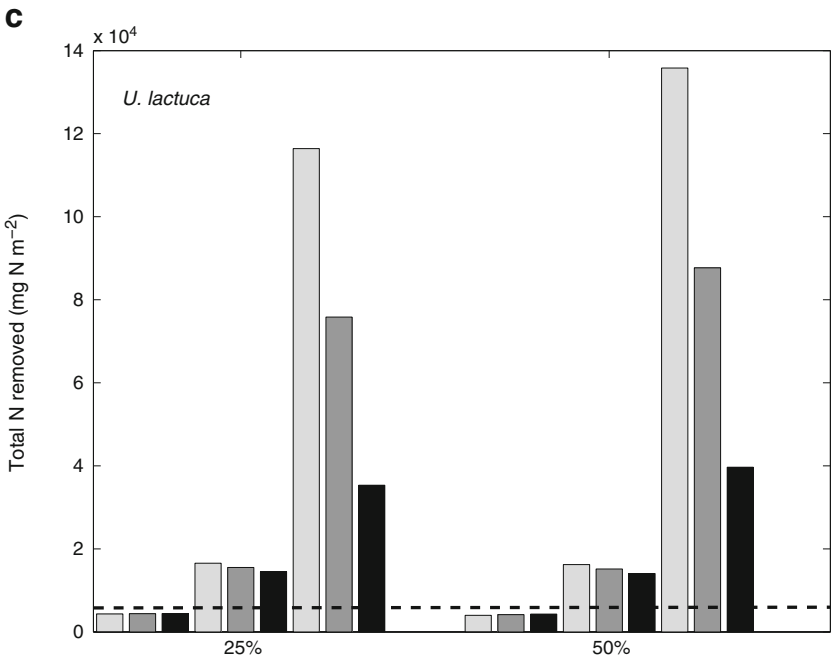

Fig. 7 (continued)

rate is an end-of-season increase in total N for *U. lactuca* and decrease for the other two species. Of the species investigated, *U. lactuca* has the highest growth rate and is able to reach the biomass required to remove DIN at a rate that enables it to surpass the growth rate at the lower flow regime. Al-Hafedh et al. (2014) found that increasing the rate of effluent flow increased biomass yield for *U. lactuca*, and that flow rate was more important in this regard than stocking density.

Although *M. pyrifera* and *P. umbilicalis* showed reduced bioremediation capacity, as flow rate increased after March, total N increased faster under higher flow for both. This may be due to the seasonal increase in background DIN. Although maximum growth rate is important in achieving the biomass required to remove the DIN under higher flow, it is not the only element important in optimizing DIN removal in the model. *P. umbilicalis* has a higher maximum growth rate (μ) than *M. pyrifera*; however, the latter species was less sensitive to the change in flow when comparing end-of-season total N. The reason for this may be in the uptake term in Eq. (3). Here, uptake depends partly on the ratio of algal height to water depth h_{MA}/z. For *M. pyrifera*, this term is always increasing; however, in general, there will eventually be a limit to how fast the flow can be before DIN is washed away and before the algae can take it up. Hepburn et al. (2007) found that *M. pyrifera* had greater growth rates at wave-exposed sites than at sheltered sites. Faster flow can reduce the boundary layer around the macroalgae blades increasing the uptake (Wheeler 1980), although our model does not explicitly model DIN uptake dependent on boundary layer dynamics. Future models may need to incorporate a mechanistic term relating flow and uptake to further understand this dynamic.

Optical depth

For both *U. lactuca* and *P. umbilicalis*, an increase in light attenuation resulted in reduced growth rate from April (autumn) to August (late winter). This result is more pronounced for *P. umbilicalis*. *M. pyrifera* showed highest growth at K_d=0.6 m^{-1} and lowest at K_d=0.2 m^{-1}, which we interpret to indicate photoinhibition, limiting growth when light attenuation is low. *M. pyrifera* has the lowest saturation point (I_s) of our three species. If the value of I_s for *M. pyrifera* is increased to that of *U. lactuca*, then it displays the same relationship between optical depth and growth as do the two smaller species (results not shown; I_s is the parameter that determines the magnitude of photoinhibition on macroalgal growth). The results at the high to midrange of optical depth for *M. pyrifera* imply that although optical depth may reduce photoinhibition, there is a point when light levels become too low and growth is reduced. As *M. pyrifera* was allowed to increase its height, in summer where it would be close to the surface, the potential for photoinhibition should increase. However, the resultant increase in biomass should act to counter this effect through self-shading. *M. pyrifera* has been shown to be susceptible to photoinhibition, particularly at midday, when cultivated near fish farms in Chile in spring and summer (Buschmann et al. 2008). Broch and Slagstad (2012) found cultivation depth did not greatly influence

seasonal biomass for the species *Saccharina latissima* in a similar modeling approach; however, they used a K_d= 0.07 m^{-1}, which was considerably lower than the range of attenuation coefficients used here.

As fixed nitrogen increased/decreased for each species, so stored nitrogen decreased/increased for each of our optical depth experiments. The combined effect of this meant that for *U. lactuca* and *P. umbilicalis*, the total remediated nitrogen was the same at all three optical depths. This implies that the algae with lower biomass may have higher stored N content. Broch et al. (2011) use a more complex formulation for internal nutrient composition in their macroalgae model, using the internal reserves of carbon and nitrogen to dynamically determine the stoichiometric ratio of carbon to nitrogen which yielded more realistic (and perhaps more interpretable) results. Nonetheless, our simpler formulation based on Solidoro et al. (1997) is sufficient to show that the relationship between N storage and fixation will both influence the cultivation strategy for IMTA as well as having clear economic implications.

Harvesting

The establishment phase appears crucial to a successful harvesting scheme. All three algae possess a high maximal growth rate (μ) and so are able to fix N very efficiently. The key to successful bioremediation in the early stages of growth is for each species to achieve a biomass capable of removing DIN in sufficient quantities to fuel their high demands. Eventually, the biomass achieves a density where light and nutrient limitation acts to reduce their growth rate considerably. At this point, harvesting frequency becomes important as this reduces the limiting effect and thus stimulates higher growth rates. This is why total N reduced with harvesting frequency for schemes with a 30-day establishment phase but increased with harvesting frequency for those with 60- and 90-day establishment phases. This could also explain the variability in the results for H=0.25 and H=0.5. In their simple model for seaweed growth, Lee and Ang (1991) found the optimal harvest strategy had the same period as the macroalgal growth and mortality terms. We note however that unlike our system, their model treats harvesting as continuous and not a discrete process and that it does not include DIN uptake as stored N, while it does show the importance of incorporating growth rate variability with harvesting strategies.

Harvesting strategies from other studies have focused on the sustainability and/or reduction of natural populations of macroalgae and so a direct comparison with our findings is not appropriate. Kelp harvesting is also done in practice by reducing the height of the kelp and not by thinning of the plants, as was the case in our simulation. We decided on this strategy because we consider plant height to be a vital component of bioremediation. We acknowledge that in deciding on a harvesting strategy, there are many other elements to consider, including market demand, cost of harvesting, price, etc. (Troell et al. 2009). In addition, we have not considered diurnal effects on growth/uptake rates, and this may influence the time of day for harvest. In an IMTA arrangement, the diurnal profile of ammonium discharge from the salmon may affect the ambient nutrient concentrations, which in turn may also have a significant impact on harvest strategy.

Improvements to the model

Macroalgal communities in nature can fluctuate between high- and low-standing biomass due to factors such as grazing pressure, hydrodynamic losses, other seasonal forcing, or natural senescence. Our macroalgae model does not simulate a steady-state biomass subject to long-term population dynamics but an increasing biomass grown under optimal conditions. Of the modifying factors just mentioned, mechanical and grazing losses could theoretically be controlled, or at least better understood, in a farming context.

Natural senescence has an unavoidable effect on macroalgae losses. A recent model for age-related senescence of *M. pyrifera* fronds (Rodriguez et al. 2013) showed that progressive senescence accounted for 73 % of the variation in biomass between kelp communities. Incorporating a mortality term based on natural senescence may form part of a more realistic model and also aid in the search for an optimal harvesting scheme.

We have used the formulation of Solidoro et al. (1997) for growth dependent on the internal nitrogen quota Q. We believe this formulation was appropriate for application in this study. However, this model does not incorporate carbon uptake dynamics, which are important in representing the internal macroalgae dynamics that determine N fixation. Formulations similar to those presented by Broch et al. (2013) would be necessary to more accurately represent growth dynamics and seasonal biomass estimates. In a future study, we intend to include our model in a fully coupled 3D hydrodynamic, biogeochemical, and sediment model of the region to examine the growth dynamics of our species in a more realistic environment that includes competition with phytoplankton and sporadic access to nutrients.

Conclusion

This study shows that IMTA offers a flexible solution to bioremediation of the nutrient input into an ecosystem from finfish aquaculture. We have shown that in a near-field scenario, of the three species we considered, only the giant kelp, *M. pyrifera*, offers reasonable bioremediation of salmon farm ammonium in the absence of harvesting. Increasing water flow reduced total N removal by *M. pyrifera* (marginally) and *P. umbilicalis* over a season, while total N removal for

U. lactuca increased with water flow. Increasing optical depth increased the total N removed by *M. pyrifera* at low to moderate optical depths but had no effect on total N removed by *U. lactuca* and *P. umbilicalis*. Harvesting had a positive effect on total N removal by all three species when harvesting commenced after 60 days. The greatest removal occurred when harvesting began after 90 days with an interval of 2 weeks thereafter, and there was a minor improvement if 50 % of the biomass was removed per harvest instead of 25 %. Optimal harvesting resulted in a 20–25-fold increase in bioremediation capacity across our three species.

Acknowledgments We acknowledge Dr. Mark Baird for his generous assistance and valuable advice and the FRDC for funding part of this research.

Appendix

Table 4 Biological intermediate processes

Symbol	Equation no.	Description	Formula	Unit
$f(N,Q)$	12	Uptake of external N source into internal reserve	$\frac{V_M N}{K_{1/2}+N}\frac{Q_{max}-Q}{Q_{max}-Q_{min}}$	mg N g^{-1} dw d^{-1}
$\mu g(E,Q,T)$	13	Growth function for macroalgae	$\mu g(E)g(Q)g(T)$	d^{-1}
$g(E)$	14	Growth limitation due to light	$\frac{e}{K\times h}\left(e^{-\frac{Ez e^{-Kh}}{I_s}}-e^{-\frac{Ez}{I_s}}\right)$	Dimensionless
$g(T)$	15	Growth limitation due to temperature	$\frac{1}{1+\exp(-(T-T_0)/T_r)}$	Dimensionless
$g(Q)$	16	Growth limitation due to internal nutrient reserves	$\frac{Q-Q_{min}}{Q-k_c}$	Dimensionless
E_z	17	Irradiance at top of macroalgal canopy	$E_0 e^{-Kz}$	μmol photons m^{-2} s^{-1}
K	18	Extinction rate of light due to water and algae	K_d+K_{MA}	m^{-1}
K_{MA}	19	Extinction rate of light due to algae	$N_f a_{cs}\left(\max\left(\frac{h}{z},1\right)\right)\left(\min(h,z)^{-1}\right)$	m^{-1}
B	20	Biomass of dry macroalgae	$N_f {Q_{min}}^{-1}$	g dw m^{-3}
Q	21	Internal nutrient quota of macroalgae	$Q_{min}(1+N_s N_f^{-1})$	mg N g^{-1} dw
h_{MA}	22	Height of *Macrocystis*	$(0.00174N_f/\text{num\_fronds})^{1.047}$	m

Table 5 Parameters for the macroalgal growth model

Symbol	Description	Units	*Macrocystis*	*Ulva*	*Porphyra*
μ	Max. growth rate	d^{-1}	0.2[a]	0.45[f]	0.33[j]
V_{NH_4}	Max. uptake rate (amm.)	mg N g^{-1} dw d^{-1}	8.0[b]	124.0[f]	60.0[k]
V_{NO_3}	Max. uptake rate (nit.)	mg N g^{-1} dw d^{-1}	10.3[c]	39.0[f]	25.0[l]
K_{NH_4}	Half sat. const. (amm.)	mg N m^{-3}	74.2[b]	700.0[f]	700.0[l]
K_{NO_3}	Half sat. const. (nit.)	mg N m^{-3}	182.0[c]	70.0[f]	300.0[l]
Q_{max}	Max. internal nitrogen	mg N g^{-1} dw	25.0[a]	42.0[f]	70.0[m]
Q_{min}	Min. internal nitrogen	mg N g^{-1} dw	7.0[d]	13.0[f]	14.0[j]
K_c	Half growth const.	mg N g^{-1} dw	6.0[e]	7.0[f]	7.0[j]
T_0	Optimal temp.	°C	12.0[f]	12.0[f]	12.0[f]
T_r	Range of optimal temp.	°C	1.0[f]	1.0[f]	1.0[f]
I_S	Saturation irradiance	μmol photons m^{-2} s^{-1}	134.0[g]	200.0[f]	277.0[m]
a_{cs}	Nitrogen specific shading	m^2 mg^{-1} N	0.0001[h]	0.00033[i]	0.00036[n]
d_m	Mortality rate	d^{-1}	0.003[i]	0.003[i]	0.003[i]
h_{MA}	Height of *U. lactuca*	m	–	0.2[i]	0.2[i]
P. umbilicalis					
num_fronds	Number of fronds	Dimensionless	7.0[o]	–	–
r_L	Remineralization rate	d^{-1}	0.2[p]	0.2[p]	0.2[p]

Table 5 (continued)

Symbol	Description	Units	*Macrocystis*	*Ulva*	*Porphyra*
r_N	Nitrification rate	d^{-1}	0.1[p]	0.1[p]	0.1[p]
λ_R	Refresh rate	d^{-1}	0.25[o]	0.25[o]	0.25[o]
K_d	Light attenuation coefficient	m^{-1}	0.1[p]	0.1[p]	0.1[p]

[a] Zimmerman and Kremer (1984)

[b] Haines and Wheeler (1978)

[c] Gerard (1982)

[d] Lobban and Harrison (1994)

[e] Hernandez-Carmona et al. (2001)

[f] Solidoro et al. (1997)

[g] Buschmann et al. (2008)

[h] Enriquez et al. (1994)

[i] Trancoso et al. (2005)

[j] Hafting (1999)

[k] Johansson and Snoeijs (2002)

[l] Pedersen et al. (2004)

[m] Carmona et al. (2006) and Pedersen et al. (2004)

[n] Markager and Sand-Jensen (1996)

[o] Calibration

[p] Wild-Allen et al. (2010)

References

Aldridge JN, Trimmer M (2009) Modelling the distribution and growth of 'problem' green seaweed in the Medway estuary, UK. Hydrobiologia 629:107–122

Al-Hafedh YS, Alam A, Buschmann AH (2014) Bioremediation potential, growth and biomass yield of the green seaweed. Ulva lactuca in an integrated marine aquaculture system at the Red Sea coast of Saudi Arabia at different stocking densities and effluent flow rates. Rev Aquac. doi:10.1111/raq.12060

Broch OJ, Slagstad D (2012) Modelling seasonal growth and composition of the kelp *Saccharina latissima*. J Appl Phycol 24:759–776

Broch OJ, Ellingsen IH, Forbord S, Wang X, Zsolt V, Alver MO, Skjermo J (2013) Modelling the cultivation and bioremediation potential of the kelp *Saccharina latissima* in close proximity to an exposed salmon farm in Norway. Aquac Env Interact 4:187–206

Bruhn A, Dahl J, Nielsen HB, Nikolaisen L, Rasmussen MB, Markager S, Jensen PD (2011) Bioenergy potential of *Ulva Lactuca*: biomass yield, methane production and combustion. Bioresour Technol 102: 2595–2604

Buschmann AH, Varela DA, Hernandez-Gonzalez MC, Huovinen P (2008) Opportunities and challenges for the development of an integrated seaweed-based aquaculture activity in Chile: determining the physiological capabilities of *Macrocystis* and *Gracilaria* as biofilters. J Appl Phycol 20:571–577

Carmona R, Kraemer GP, Yarish C (2006) Exploring Northeast American and Asian species of *Porphyra* for use in an integrated finfish–algal aquaculture system. Aquaculture 252:54–65

Chopin T, Yarish C, Wilkes R, Belyea E, Lu S, Mathieson A (1999) Developing *Porphyra*/salmon integrated aquaculture for bioremediation and diversification of the aquaculture industry. J Appl Phycol 11:463–472

Clementson LA, Parslow JS, Turnbull AR, Bonham PI (2004) Properties of light absorption in a highly coloured estuarine system in southeast Australia which is prone to blooms of the toxic dinoflagellate *Gymnodinium catenatum*. Estuar Coast Shelf Sci 60:101–112

CSIRO (2009) CSIRO Atlas of Regional Seas (CARS), from http://www.marine.csiro.au/~dunn/cars2009/.

ElkhornSlough.org (2012). Elkhorn slough plants: sea lettuce, from http://www.elkhornslough.org/sloughlife/plants/sea_lettuce.htm.

Enriquez S, Agusti S, Duarte CM (1994) Light absorption by marine macrophytes. Oecologia 98:121–129

Everett JD, Baird ME, Suthers IM (2007) Nutrient and plankton dynamics in an intermittently closed/open lagoon, Smiths Lake, southeastern Australia: an ecological model. Estuar Coast Shelf Sci 72: 690–702

Gerard VA (1982) In situ water motion and nutrient uptake by the giant kelp *Macrocystis pyrifera*. Mar Biol 69:51–54

Hafting JT (1999) Effect of tissue nitrogen and phosphorus quota on growth of *Porphyra yezoensis* blades in suspension cultures. Hydrobiologia 398/399:305–314

Haines KC, Wheeler PA (1978) Ammonium and nitrate uptake by the marine macrophytes *Hypnea musciformis* (Rhodophyta) and *Macrocystis pyrifera* (Phaeophyta). J Phycol 14:319–324

Hepburn CD, Holborow JD, Wing SR, Frew RD, Hurd CL (2007) Exposure to waves enhances the growth rate and nitrogen status of the giant kelp *Macrocystis pyrifera*. Mar Ecol Prog Ser 339:99–108

Hernandez-Carmona C, Robledo D, Serviere-Zaragoza E (2001) Effect of nutrient availability on *Macrocystis pyrifera* recruitment and survival near its southern limit off Baja California. Bot Mar 44:221–229

Hernández I, Martínez-Aragón JF, Tovar A, Pérez-Lloréns JL, Vergara JJ (2002) Biofiltering efficiency in removal of dissolved nutrients by three species of estuarine macroalgae cultivated with sea bass (*Dicentrarchus labrax*) waste waters 2. Ammonium. J Appl Phycol 14:375–384

Hernandez I, Fernandez-Engo MA, Perez-Llorens JL, Vergara JJ (2005) Integrated outdoor culture of two estuarine macroalgae as biofilters for dissolved nutrients from *Sparus aurata* waste waters. J Appl Phycol 17:557–567

Johansson G, Snoeijs P (2002) Macroalgal photosynthetic responses to light in relation to thallus morphology and depth zonation. Mar Ecol Prog Ser 244:63–72

Lee CS, Ang P Jr (1991) A simple model for seaweed growth and optimal harvesting strategy. Ecol Model 55:67–74

Lobban CS, Harrison PJ (1994) Seaweed ecology and physiology. Cambridge University Press, Cambridge

Markager S, Sand-Jensen K (1996) Implications of thallus thickness for growth-irradiance relationships of marine macroalgae. Eur J Phycol 31:79–87

MarLIN. (2012). Purple laver—*Porphyra umbilicalis*, from http://www.marlin.ac.uk/speciesinformation.php?speciesID=4194

Neori A, Cohen I, Gordin H (1991) *Ulva lactuca* biofilters for marine fishpond effluents. II. Growth rate, yield and C:N ratio. Bot Mar 34: 483–489

North WJ, Jackson GA, Manley SL (1986) *Macrocystis* and its environment, knowns and unknowns. Aquat Bot 26:9–26

Pedersen A, Kraemer G, Yarisha C (2004) The effects of temperature and nutrient concentrations on nitrate and phosphate uptake in different species of *Porphyra* from Long Island Sound (USA). J Exp Mar Biol Ecol 312:235–252

Ren JS, Stenton-Dozey J, Plew DR, Fang J, Gall M (2012) An ecosystem model for optimising production in integrated multitrophic aquaculture systems. Ecol Model 246:34–46

Robertson-Andersson DV, Potgieter M, Hansen J, Bolton JJ, Troell M, Anderson R, Probyn T (2008) Integrated seaweed cultivation on an abalone farm in South Africa. J Appl Phycol 20:579–595

Rodriguez GE, Rassweiler A, Reed DC, Holbrook SJ (2013) The importance of progressive senescence in the biomass dynamics of giant kelp (*Macrocystis pyrifera*). Ecology 94:1848–1858

Rykiel EJ (1995) Testing of ecological models: the meaning of validation. Ecol Model 90:229–244

Sanderson JC, Di Benedetto R (1988) Tasmanian seaweeds for the edible market Department of Sea Fisheries Technical report. Marine Laboratories Department of Sea Fisheries, Hobart, Tasmania

Sanderson JC, Cromey CJ, Dring MJ, Kelly MS (2008) Distribution of nutrients for seaweed cultivation around salmon cages at farm sites in north-west Scotland. Aquaculture 278:60–68

Silva C, Yanez E, Martin-Diaz ML, DelValls TA (2012) Assessing a bioremediation strategy in a shallow coastal system affected by a fish farm culture—application of GIS and shellfish dynamic models in the San Pedro, SW Spain. Mar Pollut Bull 64:751–765

Solidoro C, Pecenik G, Pastres R, Franco D, Dejak C (1997) Modelling macroalgae (*Ulva rigida*) in the Venice lagoon: model structure identification and first parameters estimation. Ecol Model 94:191–206

Thompson PA, Bonham P, Wilcox S, Crawford C (2005) Baseline monitoring in D'Entrecasteaux Channel Technical report. CSIRO Marine and Atmospheric Research, Hobart, Tasmania

Trancoso AR, Saraiva S, Fenandes L, Pina P, Leitao P, Neves R (2005) Modelling macroalgae using a 3D hydrodynamic-ecological model in a shallow, temperate estuary. Ecol Model 187:232–246

Troell M, Joyce A, Chopin T, Neori A, Buschmann AH, Fang JG (2009) Ecological engineering in aquaculture—potential for integrated multi-trophic aquaculture (IMTA) in marine offshore systems. Aquaculture 297:1–9

Utter BD, Denny MW (1996) Wave-induced forces on the giant kelp *Macrocystis pyrifera* (Agardh): field test of a computational model. J Exp Biol 199:2645–2654

Wang X, Olsen LM, Reitan KI, Olsen Y (2012) Discharge of nutrient wastes from salmon farms: environmental effects, and potential for integrated multi-trophic aquaculture. Aquac Env Interact 2:267–283

Wheeler WN (1980) Effect of boundary layer transport on the fixation of carbon by the giant kelp *Macrocystis pyrifera*. Mar Biol 56: 103–10

Wild-Allen K, Herzfeld M, Thompson PA, Rosebrock U, Parslow J, Volkman JK (2010) Applied coastal biogeochemical modelling to quantify the environmental impact of fish farm nutrients and inform managers. J Mar Syst 81:134–147

Yokoyama H, Ishihi Y (2010) Bioindicator and biofilter function of *Ulva spp*. (Chlorophyta) for dissolved inorganic nitrogen discharged from a coastal fish farm—potential role in integrated multi-trophic aquaculture. Aquaculture 310:74–83

Zimmerman RC, Kremer JN (1984) Episodic nutrient supply to a kelp forest ecosystem in Southern California. J Mar Res 42:591–604